pH-Response Mechanism of p-Aminobenzenethiol on Ag Nanoparticles Revealed By Two-Dimensional Correlation Surface-Enhanced Raman Scattering Spectroscopy

ARTICLE *in* JOURNAL OF PHYSICAL CHEMISTRY LETTERS · NOVEMBER 2012

Impact Factor: 7.46 · DOI: 10.1021/jz301428e

6 AUTHORS, INCLUDING:

Wei Ji
Dalian University of Technology
30 PUBLICATIONS **363** CITATIONS
SEE PROFILE

Nicolas Spegazzini
Massachusetts Institute of Technology
23 PUBLICATIONS **99** CITATIONS
SEE PROFILE

Bing Zhao
Jilin University
275 PUBLICATIONS **5,010** CITATIONS
SEE PROFILE

Yukihiro Ozaki
Kwansei Gakuin University
916 PUBLICATIONS **17,729** CITATIONS
SEE PROFILE

THE JOURNAL OF PHYSICAL CHEMISTRY Letters

Letter

pubs.acs.org/JPCL

pH-Response Mechanism of *p*-Aminobenzenethiol on Ag Nanoparticles Revealed By Two-Dimensional Correlation Surface-Enhanced Raman Scattering Spectroscopy

Wei Ji,[†] Nicolas Spegazzini,[‡] Yasutaka Kitahama,[‡] Yujing Chen,[‡] Bing Zhao,*[,†] and Yukihiro Ozaki*[,‡]

[†]State Key Laboratory of Supramolecular Structure and Materials, Jilin University, Changchun 130012, P. R. China

[‡]Department of Chemistry, School of Science and Technology, Kwansei Gakuin University, Sanda, Hyogo 669-1337, Japan

Supporting Information

ABSTRACT: The existence of pH-dependent surface-enhanced Raman scattering (SERS) of *p*-aminobenzenethiol (PATP) on Ag nanoparticles has been confirmed by numerous studies, but its mechanism still remains to be clarified. Discussion of the mechanism is at a standstill because of the lack of a systematic investigation of the process behind the pH-induced variation of the PATP behavior. Two-dimensional correlation spectroscopy is one of the most powerful and versatile spectral analysis methods for investigating perturbation-induced variations in dynamic data. Herein, we have analyzed the pH-dependent behavior of PATP using a static buffer solution with pH ranging from 3.0 to 2.0. The order of the variations in the different vibrational intensities was carefully investigated based on 2D correlation SERS spectroscopy. These results have demonstrated that the very first step of the pH-response process involves protonation of the amine group. The pH-response mechanism revealed is an important new component to our understanding of the origin of the b_2-type bands of PATP.

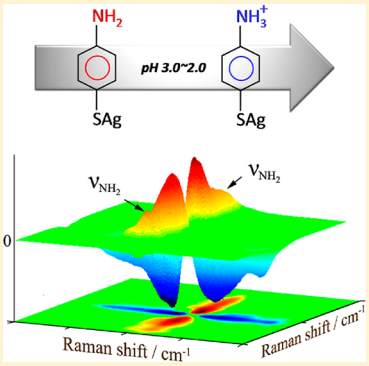

SECTION: Spectroscopy, Photochemistry, and Excited States

In recent years, intense interest in the field of surface-enhanced Raman scattering (SERS) has been focused on its biological and environmental applications.[1−5] As the use of analysis and detection technique based on SERS have spread, the attempts to understand further the enhancement mechanism have continued, and explaining this mechanism has become an increasingly urgent problem.[6−9] The electromagnetic and chemical enhancement mechanism are the two primary mechanisms responsible for the huge enhancement in SERS. The former is associated with the resonant excitation of the surface plasmon in nanoparticles and is independent of the molecular effects (structure, energy levels, etc.).[10−12] The development of nanoscience has enabled researchers to develop the theory of electromagnetic enhancement in its entirety. However, the latter mechanism involves a photoinduced charge-transfer (CT) transition between the Fermi level of the substrate and the molecular energy level in a different system.[13−17] Therefore, it is difficult to determine the magnitude of the CT contribution, and this mechanism remains a matter of controversy.

p-Aminobenzenethiol (PATP) is one of the most popular molecules in the study of the chemical enhancement mechanism because of its high-quality signal and unusual performance.[18−37] Its SERS spectrum is affected by many factors, such as the substrate materials, excitation wavelengths, testing environments, and so on. The b_2-type bands of PATP located at 1573, 1440, 1391, and 1142 cm^{-1} have been considered as evaluation indexes of the CT contribution to SERS.[18−25] However, recently questions have been raised that dispute about the origin of the b_2-type bands. Some researchers have argued that the so-called b_2-type bands of PATP actually arise from the a_g modes of 4,4′-dimercaptoazobenzene (4,4′-DMAB), which is formed by a catalytic coupling reaction on metal substrates.[32−34,38] Other researchers have demonstrated that the b_2-type bands have nothing to do with surface-induced photoreaction products like 4,4′-DMAB.[23−31,35,37,39] They observed many different phenomena by varying the substrate materials and the testing conditions (e.g., temperature, excitation wavelength, solution pH, and gas environment) and found the results to be puzzling in terms of the photoreaction but easily understood in terms of the CT enhancement mechanism.

In these works, the pH-dependent behavior of PATP is one of the decisive factors. Thus, there has been intense discussion on this phenomenon.[31,40,41] The b_2-type band intensities decreased with decreasing solution pH and could be reversibly tuned using the solution pH. Photoinduced CT supporters consider this phenomenon to be caused by protonation and deprotonation of the amine group.[28,31] The protonation of the amine group improves the orbital level of PATP and thus hinders the degree of CT, leading to the decrease in the b_2-type band intensities through the Herzberg−Teller contribution.[28]

Received: September 15, 2012
Accepted: October 17, 2012
Published: October 17, 2012

   dx.doi.org/10.1021/jz301428e | *J. Phys. Chem. Lett.* 2012, 3, 3204−3209

However, the surface-induced photoreaction supporters insist that PATP is apt to be catalyzed into 4,4′-DMAB because of its high mobility in the basic solution, which could also result in the pH-dependent behavior.[34,40,41] Meanwhile, the reversible behavior of the a_g modes of 4,4′-DMAB suggests that 4,4′-DMAB can diffuse into or out of the hotspot.[34] With the current information, it is very difficult to reach a convincing conclusion. The discussion is apparently at a standstill because of the lack of a systematic study of the pH-response process.

Since the proposal of generalized 2D correlation spectroscopy by Noda in 1993, it has been applied extensively to investigate the conformations and dynamics of various molecular systems including proteins, peptides, and polymers.[42−46] It allows one to decompose highly overlapping bands into individual components and enhance the spectral resolution, which allows the interactions and dynamics of information of functional groups of the system to be monitored. In recent years, 2D correlation SERS spectroscopy has been developed, and it has quickly become an important analytical method for characterizing protein structures and dynamics and analyzing the continuum in single-molecule SERS spectra.[47−52] Two-dimensional correlation spectroscopy is one of the most powerful and versatile spectral analysis methods for investigating perturbation-induced variations in dynamic data.[44,53,54] Thus, the pH-induced variations of the PATP behavior can be studied in much greater detail using 2D correlation spectroscopy. It was clearly found that the very first step of the pH-response process involves a protonation of the amine group. Moreover, a decay time exists in the pH-response process that is due to the diffusion of the H^+ ions in the buffer solution. These results can help us to assess the pH-response mechanism and consequently understand the true origin of the b_2-type SERS bands of PATP.

To study further the details of the pH response process of PATP, a static buffer solution was used in the pH response experiment. Figure 1 shows the SERS spectra of PATP obtained by immersing the substrate in a pH 2.0 buffer solution. The most notable result is that the band intensities

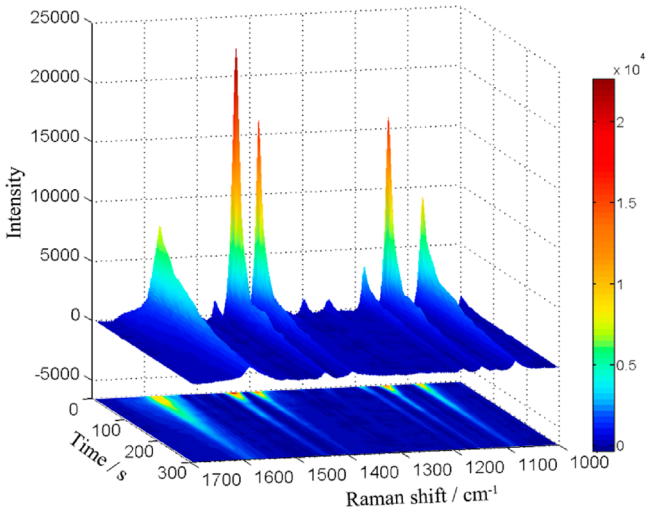

Figure 1. Representative SERS spectra of PATP on an Ag nanoparticle as a function of exposure time. The spectra were obtained by immersing the substrate in a pH 2.0 buffer solution. The integration time for each spectrum was 10 s. A corresponding cloud map is shown under the SERS spectra.

decreased as the exposure time increased. However, the decay rates for these bands are different from each other. Obviously, the decreases in the intensities of the bands at 1146, 1391, 1438, and 1576 cm^{-1} are faster than those of the bands at 1078 and 1587 cm^{-1}. (See the cloud map in Figure 1.) For detailed analysis, the variations in the intensities of the typical bands at 1078, 1146, 1391, and 1438 cm^{-1} are shown in Figure 2. As expected, there is a decay time in the pH-response process that is caused by many factors such as the thermal effect of the laser, adsorbate mobility, and diffusion of H^+ ions in the buffer solution. (See Figure S1 of the Supporting Information.)[55] It should be pointed out that selective decreases in the intensities of the bands at 1078, 1146, 1391, and 1438 cm^{-1} relative to the other bands are typical features of the pH-response process. The relative intensities underwent pronounced loss as the exposure time increased and finally achieved an equilibrium state after 120 s of illumination (Figure 2B).

The SERS spectrum reached an equilibrium state after 120s of laser illumination, after which further SERS spectra were measured in the range of 120−150 s. Figure 3 shows the SERS spectra of PATP obtained by immersing the substrate into different pH buffer solutions. The same trend was observed as the pH decreased; the intensities of the bands at 1146, 1391, 1438, and 1576 cm^{-1} decreased faster than the other bands. In general, these bands are assigned to b_2 modes whose intensities are borrowed from CT transitions between a PATP molecule and an Ag nanoparticle.[6,18] Recently, many researchers have argued that the so-called b_2-type bands are selectively enhanced under some conditions and that these bands do not arise from the Herzberg−Teller contribution to SERS at all but rather from the a_g modes of 4,4′-DMAB produced from the PATP.[32,38] Under such circumstances, it is not easy to determine the origin of these bands. Therefore, the exploration of the pH-dependent SERS spectra requires a more advanced tool such as 2D correlation spectroscopy.

Figure 4 shows the synchronous and asynchronous 2D correlation maps calculated using the SERS spectra of PATP measured in the different pH buffer solutions. The synchronous map shows positive correlation peaks centered at (1079, 1587 cm^{-1}), (1146, 1587 cm^{-1}), (1392, 1587 cm^{-1}), (1438, 1587 cm^{-1}), and (1576, 1587 cm^{-1}) (see red dotted line in Figure 4A), which suggest that the intensities of the SERS peaks decrease as the pH decreases. However, the corresponding correlation peaks on the asynchronous map are negative. According to Noda's rules,[53] the different signs of the corresponding synchronous and asynchronous correlation features indicate that the changes in the other bands are delayed relative to the change in the 1587 cm^{-1} band. Regardless of which molecule is considered to produce the band at 1587 cm^{-1}, it can be clearly attributed to the benzene skeleton vibration.[18,32] Consequently, the first step of the pH-response process involves an rearrangement of the electronic cloud of the benzene ring that results in a change in the CC skeleton vibration.

It should be worth nothing that the band at 1079 cm^{-1} can be unambiguously attributed to the C−S stretching vibration.[18,32] The cross-peaks centered at (1079, 1146 cm^{-1}), (1079, 1392 cm^{-1}), and (1079, 1438 cm^{-1}) are positive in the asynchronous map, indicating that the C−S stretching band changes earlier than the bands at 1146, 1392, and 1438 cm^{-1} in the pH-response process. However, there is still no clue as to the reason for the rearrangement of the electronic cloud of the benzene ring that occurs as the pH decreases. As we all know,

dx.doi.org/10.1021/jz301428e | J. Phys. Chem. Lett. 2012, 3, 3204−3209

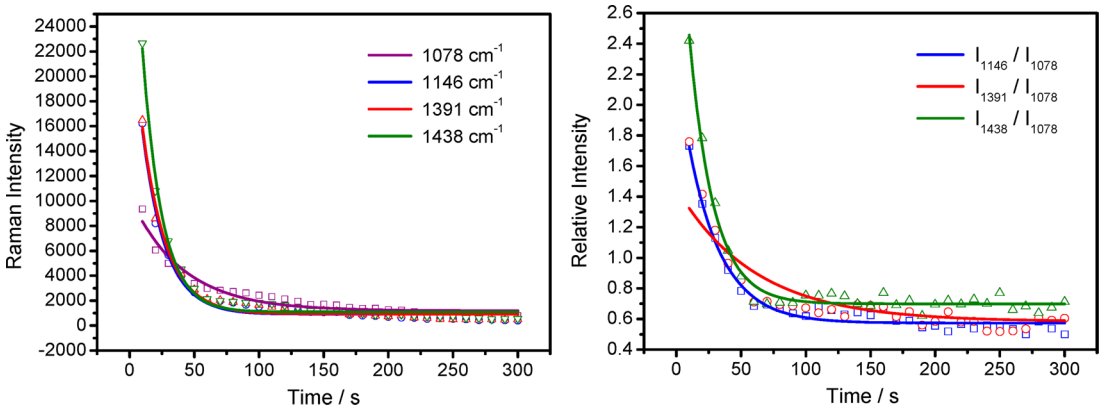

Figure 2. Variations in intensities of the main bands at 1078, 1146, 1391, and 1438 cm^{-1} in a SERS spectrum of PATP on Ag nanoparticles as a function of illumination time. (A) Decay profiles were obtained by immersing the substrate in a pH 2.0 buffer solution. (B) Corresponding intensities relative to the intensity of the 1078 cm^{-1} band.

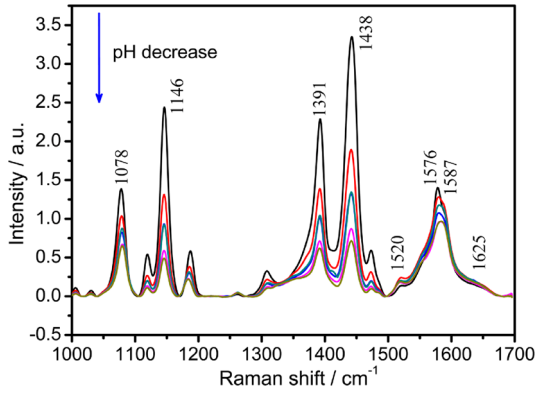

Figure 3. SERS spectra of PATP on Ag nanoparticles at various pH values ranging from pH 3.0 to 2.0 in steps of 0.20 pH units. All SERS spectra were normalized using the silicon wafer band at 520.7 cm^{-1}.

there is abundant information in the region of 1500−1700 cm^{-1}. Nevertheless, because of the heavy overlap of the various vibrational bands and the much stronger intensity of the CC vibration band at 1587 cm^{-1} compared with those of the other bands, direct interpretation of these bands provides only limited information. Therefore, this region has seldom been analyzed, and it is merely pointed out that there are two CC vibration bands in this region. Fortunately, the 2D correlation SERS spectrum is a powerful tool for analyzing the overlapping bands.

The enlarged 2D correlation SERS spectrum in the 1500−1700 cm^{-1} region is very interesting and pronounced, as shown in Figure 5. Five bands can be clearly identified at 1520, 1554, 1576, 1587, and 1625 cm^{-1}, respectively. The bands at 1625 and 1520 cm^{-1} are due to characteristic rocking vibrations of the NH_2 group. The order of the intensity changes in the two bands is listed in Table 1. It is worth noting that the intensity variations in the bands at 1625 and 1520 cm^{-1} take place before those of the bands at 1576 and 1587 cm^{-1}. This indicates that the change in the NH_2 group occurs before those in the CC bands at 1576 and 1587 cm^{-1}. Moreover, an unexpected band appears at 1554 cm^{-1}, which has appeared at exactly this location in many reports.[39,56] However, this band has not been clearly attributed to any vibration. From the asynchronous map, it can be seen that the corresponding correlations at (1554, 1625 cm^{-1}), (1554, 1520 cm^{-1}), and (1625, 1520 cm^{-1}) do not

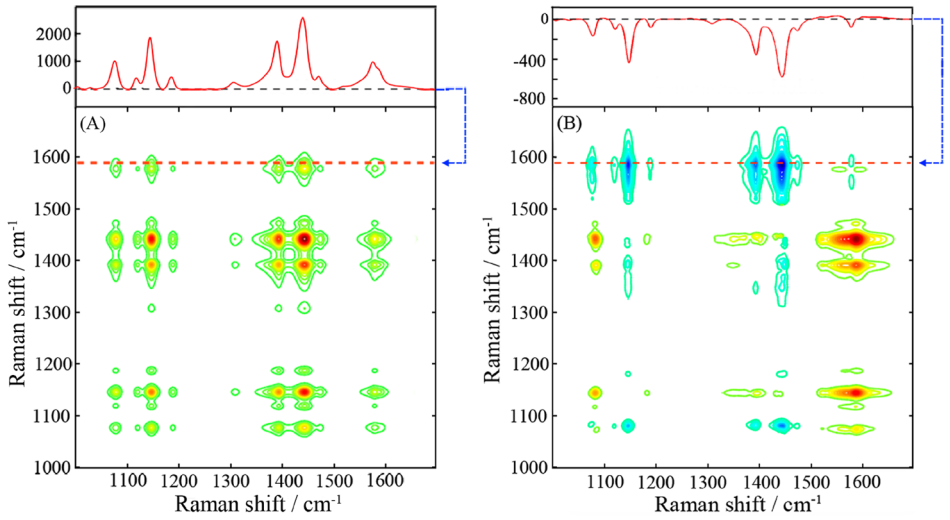

Figure 4. (A) Synchronous and (B) asynchronous 2D correlation maps of SERS spectra calculated at various pH values ranging from pH 3.0 to 2.0 in steps of 0.20 pH units. The spectral profiles above the 2D maps are cross sections of the 2D correlation maps at 1587 cm^{-1} (red horizontal line). The negative asynchronous peaks are shown in blue.

dx.doi.org/10.1021/jz301428e | J. Phys. Chem. Lett. 2012, 3, 3204−3209

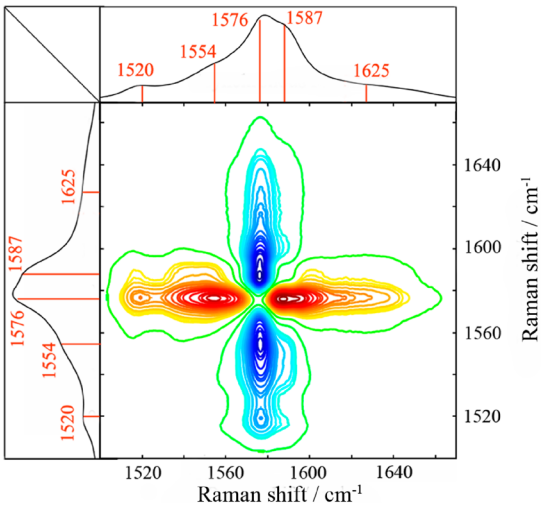

Figure 5. Enlarged asynchronous 2D correlation map in the 1500–1700 cm^{-1} region.

Table 1. Synchronous and Asynchronous Correlation Intensities and the Order of Intensity Changes of Two Bands[a]

number	Φ	Ψ	order
1	Φ(1520, 1576) > 0	Ψ(1520, 1576) > 0	1552 cm^{-1} before 1576 cm^{-1}
2	Φ(1520, 1587) > 0	Ψ(1520, 1587) > 0	1520 cm^{-1} before 1587 cm^{-1}
3	Φ(1554, 1576) > 0	Ψ(1554, 1576) > 0	1554 cm^{-1} before 1576 cm^{-1}
4	Φ(1554, 1587) > 0	Ψ(1554, 1587) > 0	1554 cm^{-1} before 1587 cm^{-1}
5	Φ(1576, 1587) > 0	Ψ(1576, 1587) < 0	1576 cm^{-1} after 1587 cm^{-1}
6	Φ(1625, 1576) > 0	Ψ(1625, 1576) > 0	1625 cm^{-1} before 1576 cm^{-1}
7	Φ(1625, 1587) > 0	Ψ(1625, 1587) > 0	1625 cm^{-1} before 1587 cm^{-1}
8	Φ(1520,1554)	Ψ(1520,1554)	none
9	Φ(1520,1625)	Ψ(1520,1625)	none
10	Φ(1554,1625)	Ψ(1554,1625)	none

[a] ν_1 after (before) ν_2 means the intensity change of the band at ν_1 occurs at a higher (lower) pH than that at ν_2.

appear, which suggests that these bands experience completely synchronous changes. Therefore, it is very likely that the change in the band intensity at 1554 cm^{-1} is associated with the NH_2 group.

Overall, on the basis of the analysis of synchronous and asynchronous maps, one can conclude that the sequential order of these bands is 1625, 1554, and 1520 cm^{-1} > 1587 cm^{-1} > 1576 cm^{-1} > 1079 cm^{-1} > 1145, 1392, and 1438 cm^{-1}. This variation order strongly suggests that the pH dependence of the SERS spectra is closely related to the change in the NH_2 group and the electronic cloud rearrangement of the benzene ring. Thus, the question arises as to what is responsible for these experimental observations related to the pH dependence of the SERS.

The pH dependence of the SERS is consistent with recent studies.[31,41,56] However, the mechanism of the pH-dependent behavior of PATP is contentious. Here we specify the differences between the two possible mechanisms and reconsider them based on the results of 2D correlation spectroscopy results. Both 4,4′-DMAB and PATP are considered. First, we assume that the SERS signals arise from 4,4′-DMAB produced from the PATP. Taking into account the fact that the molecule is more-or-less mobile on the surface as the H^+ ion concentration increases, 4,4′-DMAB may diffuse out of the hotspot, giving rise to the decrease in the corresponding intensities of the SERS peaks.[34,57] There is actually a decay time in our system, which may be due to the use of the still buffer system that limits the rate of pH-response process. This decay time suggests that the interpretation that the SERS signals arise from 4,4′-DMAB diffusing out of the hot spot seems logical. Nevertheless, the existence of asynchronous correlation features in Figure S2 in the Supporting Information is evidence against this assumption because a simple composition change alone yields only synchronous correlation peaks but not asynchronous peaks. If the composition change gives rise to a strictly proportional change in band intensity, then the corresponding asynchronous correlation intensity should be zero. The 4,4′-DMAB usually shows pH-independent behavior. The reversible SERS spectra were observed under different pH; it also suggests that there is no 4,4′-DMAB formation during the measurements.[31] Even if 4,4′-DMAB responds to H^+ ions, it is difficult to imagine how this behavior could explain the order of the intensity variation determined using the correlation peaks. Consequently, the pH-dependent behavior cannot be simply explained by the molecular diffusion. In fact, a change in the structure of the PATP molecule leads to rearrangement of electronic cloud on the benzene ring as the H^+ ion concentration increases.

On the basis of the analysis above, the pH-dependent SERS behavior cannot be convincingly interpreted using only molecular diffusion. However, the phenomena can be easily understood if the SERS signals stem from PATP. The analysis of the synchronous and asynchronous maps demonstrates that the very first step involves a change in the amine group (at 1625, 1554, and 1520 cm^{-1}) as the pH decreases, indicating that protonation of the amine group occurs first. This type of interaction gives rise to the rearrangement of the electronic cloud of the benzene ring because the LUMO energy level is sensitive to the electronic charge of the amine nitrogen atom. The variation of the electronic cloud on the benzene ring hinders the CT transition between PATP and the Ag nanoparticle, resulting in a decrease in the intensity of the b_2-type bands at 1145 (δ_{CH}), 1392 (ν_{CC} + δ_{CH}), and 1438 (ν_{CC} + δ_{CH}) cm^{-1} through the Herzberg–Teller contribution via CT. The kinetic mechanism of the pH response is shown Scheme 1.

Scheme 1. pH-Response Mechanism of *p*-Aminobenzenethiol on Ag Nanoparticles

Protonation of amine group → rearrangement of electronic cloud on benzene ring → decrease in the b_2-type band intensities through the Herzberg-Teller contribution

Protonation is a typical amine feature because the amine has a lone-pair electron that can bind a hydrogen ion to form an ammonium ion. However, the lone-pair electrons of aromatic amines are conjugated into the benzene ring, which diminishes their tendency to engage in hydrogen bonding. In our experiment, although the substrate was immersed in the buffer solution for a long time, only slight changes in the relative intensities of the PATP peaks (these data are not shown) were observed. However, it was found that significant changes in the relative band intensities occurred when the laser illuminated the

dx.doi.org/10.1021/jz301428e | J. Phys. Chem. Lett. 2012, 3, 3204–3209

substrate. This is probably related to the electrons excited from the Ag nanoparticle to the molecule that disturbs the equilibrium electron conjugation in the benzene ring and consequently promotes the protonation of the amine group. The local change in the H^+ concentration at the Ag surface is significantly greater than that in the bulk solution. The decay time may be caused by diffusion of ions from the buffer solution to the Ag surface. In the pH-response process, a red shift of the PATP vibration band occurs as the exposure time increases, which also suggests the protonation of the amine group (Figure S3 in the Supporting Information).

In conclusion, the pH-response mechanism of PATP on Ag nanoparticles has been investigated using 2D correlation SERS spectroscopy. We have found that the very first step of the response process involves the protonation of the amine group. This protonation results in rearrangement of the electronic cloud of the benzene ring that subsequently changes the ring skeleton vibration. Finally, the variations spread to the C−S and C−H vibrations. This evolution cannot be simply explained by the molecular diffusion. Rather, it is a significant H^+ ions response in which the relative decrease in the intensities of the b_2-type bands (at 1145, 1392, and 1438 cm^{-1}) in the SERS spectra occurs through the Herzberg−Teller contribution via CT. Moreover, there is a decay time in the pH-response process that may result from the diffusion of H^+ ions in the buffer solution. The electrons excited from the Ag nanoparticle to the molecule by the laser disturb the equilibrium electron conjugation in the benzene ring and promote the protonation of the amine group. Overall, the described pH-response mechanism affords new insights in the debate about the origin of the b_2-type bands in the SERS spectrum of PATP.

■ ASSOCIATED CONTENT

Supporting Information

Experimental section and 2D correlation spectrum measured in a pH 2.0 buffer solution during continuous exposure, and corresponding SERS trajectories. This material is available free of charge via the Internet at http://pubs.acs.org.

■ AUTHOR INFORMATION

Corresponding Author

*E-mail: zhaob@mail.jlu.edu.cn; Fax: +86 431 8519 3421; Tel: +86 431 8516 8473 (B.Z.). E-mail: ozaki@kwansei.ac.jp; Fax: +81 79 565 9077; Tel: +81 79 565 8349 (Y.O.).

Notes

The authors declare no competing financial interest.

■ ACKNOWLEDGMENTS

This research was supported by the National Natural Science Foundation (20921003, 20973074) of P. R. China; Specialized Research Fund for the Doctoral Program of Higher Education (20110061110017); the 111 project (B06009); and the Development Program of the Science and Technology of Jilin Province (20110338).

■ REFERENCES

(1) Smith, W. E. Practical Understanding and Use Surface Enhanced Raman Scattering/Surface Enhanced Resonance Raman Scattering in Chemical and Biological Analysis. *Chem. Soc. Rev.* **2008**, *37*, 873−1076.

(2) Kneipp, K.; Moskovits, M.; Kneipp, H. *Surface-Enhanced Raman Scattering: Physics and Applications*; Springer: Bwelin, Germany, 2006.

(3) Schlucker, S. *Surface Enhanced Raman Spectroscopy: Analytical, Biophysical and Life Science Applications*; Wiley-VCH: Weinheim, Germany, 2011.

(4) Qian, X. M.; Nie, S. M. Single-Molecule and Single-Nanoparticle SERS: from Fundamental Mechanisms to Biomedical Applications. *Chem. Soc. Rev.* **2008**, *37*, 912−920.

(5) Han, X. X.; Ozaki, Y.; Zhao, B. Label-Free Detection in Biological Applications of Surface-Enhanced Raman Scattering. *TrAC, Trends Anal. Chem.* **2012**, *38*, 67−78.

(6) Lombardi, J. R.; Birke, R. L. A Unified View of Surface-Enhanced Raman Scattering. *Acc. Chem. Res.* **2009**, *42*, 734−742.

(7) Ji, W.; Xue, X. X.; Ruan, W. D.; Wang, C. X.; Ji, N.; Chen, L.; Li, Z. S.; Song, W.; Zhao, B.; Lombardi, J. R. Scanned Chemical Enhancement of Surface-Enhanced Raman Scattering Using a Charge-Transfer Complex. *Chem. Commun.* **2011**, *47*, 2426−2428.

(8) Cui, L.; Wu, D. Y.; Wang, A.; Ren, B.; Tian, Z. Q. Charge-Transfer Enhancement Involved in the SERS of Adenine on Rh and Pd Demonstrated by Ultraviolet to Visible Laser Excitation. *J. Phys. Chem. C* **2010**, *114*, 16588−16595.

(9) Morton, S. M.; Jensen, L. Understanding the Molecule-Surface Chemical Coupling in SERS. *J. Am. Chem. Soc.* **2009**, *131*, 4090−4098.

(10) VanDuyne, R. P. *Chemical and Biochemical Applications of Lasers*; Academic Press: New York, 1979; Vol. *4*.

(11) Moskovits, M. Surface-Enhanced Spectroscopy. *Rev. Mod. Phys.* **1985**, *57*, 783−826.

(12) Le Ru, E. C.; Etchegoin, P. G. *Principles of Surface-Enhanced Raman Spectroscopy and Related Plasmonic Effects*; Elsevier: Amsterdam, 2009.

(13) Lombardi, J. R.; Birke, R. L.; Lu, T.; Xu, J. Charge-Transfer Theory of Surface Enhanced Raman Spectroscopy: Herzberg–Teller Contributions. *J. Chem. Phys.* **1986**, *84*, 4174−4180.

(14) Otto, A. The 'Chemical' (Electronic) Contribution to Surface-Enhanced Raman Scattering. *J. Raman Spectrosc.* **2005**, *36*, 497−509.

(15) Moskovits, M. Surface-Enhanced Raman Spectroscopy: a Brief Retrospective. *J. Raman Spectrosc.* **2005**, *36*, 485−496.

(16) Zayak, A. T.; Hu, Y. S.; Choo, H.; Bokor, J.; Cabrini, S.; Schuck, P. J.; Neaton, J. B. Chemical Raman Enhancement of Organic Adsorbates on Metal Surfaces. *Phys. Rev. Lett.* **2011**, *106*, 083003.

(17) Ji, W.; Kitahama, Y.; Xue, X.; Zhao, B.; Ozaki, Y. Generation of Pronounced Resonance Profile of Charge-Transfer Contributions to Surface-Enhanced Raman Scattering. *J. Phys. Chem. C* **2012**, *116*, 2515−2520.

(18) Osawa, M.; Matsuda, N.; Yoshii, K.; Uchida, I. Charge Transfer Resonance Raman Process in Surface-Enhanced Raman Scattering from p-Aminothiophenol Adsorbed on Silver: Herzberg-Teller Contribution. *J. Phys. Chem.* **1994**, *98*, 12702−12707.

(19) Cao, L. Y.; Diao, P.; Tong, L. M.; Zhu, T.; Liu, Z. F. Surface-Enhanced Raman Scattering of p-Aminothiophenol on a Au(core)/Cu(shell) Nanoparticle Assembly. *ChemPhysChem* **2005**, *6*, 913−918.

(20) Zhou, Q.; Li, X. W.; Fan, Q.; Zhang, X. X.; Zheng, J. W. Charge Transfer Between Metal Nanoparticles Interconnected with a Functionalized Molecule Probed by Surface-Enhanced Raman Spectroscopy. *Angew. Chem., Int. Ed.* **2006**, *45*, 3970−3973.

(21) Sun, Z. H.; Wang, C. X.; Yang, J. X.; Zhao, B.; Lombardi, J. R. Nanoparticle Metal-Semiconductor Charge Transfer in ZnO/PATP/Ag Assemblies by Surface-Enhanced Raman Spectroscopy. *J. Phys. Chem. C* **2008**, *112*, 6093−6098.

(22) Liu, S. S.; Zhao, X. M.; Li, Y. Z.; Zhao, X. H.; Chen, M. D. Density Functional Theory Study on Herzberg-Teller Contribution in Raman Scattering from 4-Aminothiophenol-Metal Complex and Metal-4-Aminothiophenol-Metal Junction. *J. Chem. Phys.* **2009**, *130*, 234509.

(23) Uetsuki, K.; Verma, P.; Yano, T.; Saito, Y.; Ichimura, T.; Kawata, S. Experimental Identification of Chemical Effects in Surface Enhanced Raman Scattering of 4-Aminothiophenol. *J. Phys. Chem. C* **2010**, *114*, 7515−7520.

(24) Mao, Z.; Song, W.; Chen, L.; Ji, W.; Xue, X.; Ruan, W.; Li, Z.; Mao, H.; Ma, S.; Lombardi, J. R.; Zhao, B. Metal−Semiconductor

Contacts Induce the Charge-Transfer Mechanism of Surface-Enhanced Raman Scattering. *J. Phys. Chem. C* **2011**, *115*, 18378−18383.
(25) Park, W. H.; Kim, Z. H. Charge Transfer Enhancement in the SERS of a Single Molecule. *Nano Lett.* **2010**, *10*, 4040−4048.
(26) Kim, K.; Kim, K. L.; Choi, J. Y.; Shin, D.; Shin, K. S. Effect of Volatile Organic Chemicals on Surface-Enhanced Raman Scattering of 4-Aminobenzenethiol on Ag: Comparison with the Potential Dependence. *Phys. Chem. Chem. Phys.* **2011**, *13*, 15603−15609.
(27) Kim, K.; Lee, H. B.; Choi, J.-Y.; Kim, K. L.; Shin, K. S. Surface-Enhanced Raman Scattering of 4-Aminobenzenethiol in Nanogaps between a Planar Ag Substrate and Pt Nanoparticles. *J. Phys. Chem. C* **2011**, *115*, 13223−13231.
(28) Kim, K.; Shin, D.; Choi, J.-Y.; Kim, K. L.; Shin, K. S. Surface-Enhanced Raman Scattering Characteristics of 4-Aminobenzenethiol Derivatives Adsorbed on Silver. *J. Phys. Chem. C* **2011**, *115*, 24960−24966.
(29) Kim, K.; Shin, D.; Lee, H. B.; Shin, K. S. Surface-Enhanced Raman Scattering of 4-Aminobenzenethiol on Gold: the Concept of Threshold Energy in Charge Transfer Enhancement. *Chem. Commun.* **2011**, *47*, 2020−2022.
(30) Kim, K.; Yoon, J. K.; Lee, H. B.; Shin, D.; Shin, K. S. Surface-Enhanced Raman Scattering of 4-Aminobenzenethiol in Ag Sol: Relative Intensity of a_1- and b_2-Type Bands Invariant against Aggregation of Ag Nanoparticles. *Langmuir* **2011**, *27*, 4526−4531.
(31) Kim, K.; Kim, K. L.; Shin, D.; Choi, J.-Y.; Shin, K. S. Surface-Enhanced Raman Scattering of 4-Aminobenzenethiol on Ag and Au: pH Dependence of b_2-Type Bands. *J. Phys. Chem. C* **2012**, *116*, 4774−4779.
(32) Wu, D. Y.; Liu, X. M.; Huang, Y. F.; Ren, B.; Xu, X.; Tian, Z. Q. Surface Catalytic Coupling Reaction of p-Mercaptoaniline Linking to Silver Nanostructures Responsible for Abnormal SERS Enhancement: A DFT Study. *J. Phys. Chem. C* **2009**, *113*, 18212−18222.
(33) Huang, Y.; Fang, Y.; Yang, Z.; Sun, M. Can p,p′-Dimercaptoazobisbenzene Be Produced from p-Aminothiophenol by Surface Photochemistry Reaction in the Junctions of a Ag Nanoparticle−Molecule−Ag (or Au) Film? *J. Phys. Chem. C* **2010**, *114*, 18263−18269.
(34) Huang, Y. F.; Wu, D. Y.; Zhu, H. P.; Zhao, L. B.; Liu, G. K.; Ren, B.; Tian, Z. Q. Surface-Enhanced Raman Spectroscopic Study of p-Aminothiophenol. *Phys. Chem. Chem. Phys.* **2012**, *14*, 8485−8497.
(35) Liu, H.; Yang, L.; Ma, H.; Qi, Z.; Liu, J. Molecular Sensitivity of DNA-Ag-PATP Hybrid on Optical Activity for Ultratrace Mercury Analysis. *Chem. Commun.* **2011**, *47*, 9360−9362.
(36) Yoon, J. H.; Park, J. S.; Yoon, S. Time-Dependent and Symmetry-Selective Charge-Transfer Contribution to SERS in Gold Nanoparticle Aggregates. *Langmuir* **2009**, *25*, 12475−12480.
(37) Ye, J.; Hutchison, J. A.; Uji-i, H.; Hofkens, J.; Lagae, L.; Maes, G.; Borghs, G.; Van Dorpe, P. Excitation Wavelength Dependent Surface Enhanced Raman Scattering of 4-Aminothiophenol on Gold Nanorings. *Nanoscale* **2012**, *4*, 1606−1611.
(38) Huang, Y. F.; Zhu, H. P.; Liu, G. K.; Wu, D. Y.; Ren, B.; Tian, Z. Q. When the Signal Is Not from the Original Molecule To Be Detected: Chemical Transformation of para-Aminothiophenol on Ag During the SERS Measurement. *J. Am. Chem. Soc.* **2010**, *132*, 9244−9246.
(39) Kho, K. W.; Dinish, U. S.; Kumar, A.; Olivo, M. Frequency Shifts in SERS for Biosensing. *ACS Nano* **2012**, *6*, 4892−4902.
(40) Zong, S. F.; Wang, Z. Y.; Yang, J.; Cui, Y. P. Intracellular pH Sensing Using p-Aminothiophenol Functionalized Gold Nanorods with Low Cytotoxicity. *Anal. Chem.* **2011**, *83*, 4178−4183.
(41) Sun, M.; Huang, Y.; Xia, L.; Chen, X.; Xu, H. The pH-Controlled Plasmon-Assisted Surface Photocatalysis Reaction of 4-Aminothiophenol to p,p′-Dimercaptoazobenzene on Au, Ag, and Cu Colloids. *J. Phys. Chem. C* **2011**, *115*, 9629−9636.
(42) Noda, I. Generalized Two-Dimensional Correlation Method Applicable to Infrared, Raman, and Other Types of Spectroscopy. *Appl. Spectrosc.* **1993**, *47*, 1329−1336.
(43) He, Y.; Wang, G.; Cox, J.; Geng, L. Two-Dimensional Fluorescence Correlation Spectroscopy with Modulated Excitation. *Anal. Chem.* **2001**, *73*, 2302−2309.
(44) Noda, I.; Ozaki, Y. *Two-Dimensional Correlation Spectroscopy - Applications in Vibrational and Optical Spectroscopy*; John Wiley and Sons: Chichester, U.K., 2004.
(45) Zhang, J. M.; Duan, Y. X.; Sato, H.; Tsuji, H.; Noda, I.; Yan, S.; Ozaki, Y. Crystal Modifications and Thermal Behavior of Poly(L-lactic acid) Revealed by Infrared Spectroscopy. *Macromolecules* **2005**, *38*, 8012−8021.
(46) Czarnecki, M. A. Two-Dimensional Correlation Analysis of Hydrogen-Bonded Systems: Basic Molecules. *Appl. Spectrosc. Rev.* **2011**, *46*, 67−103.
(47) Moore, A. A.; Jacobson, M. L.; Belabas, N.; Rowlen, K. L.; Jonas, D. M. 2D Correlation Analysis of the Continuum in Single Molecule Surface Enhanced Raman Spectroscopy. *J. Am. Chem. Soc.* **2005**, *127*, 7292−7293.
(48) Shashilov, V.; Xu, M.; Ermolenkov, V. V.; Fredriksen, L.; Lednev, I. K. Probing a Fibrillation Nucleus Directly by Deep Ultraviolet Raman Spectroscopy. *J. Am. Chem. Soc.* **2007**, *129*, 6972−6973.
(49) Shashilov, V. A.; Lednev, I. K. 2D Correlation Deep UV Resonance Raman Spectroscopy of Early Events of Lysozyme Fibrillation: Kinetic Mechanism and Potential Interpretation Pitfalls. *J. Am. Chem. Soc.* **2008**, *130*, 309−317.
(50) Podstawka, E.; Niaura, G. Potential-Dependent Characterization of Bombesin Adsorbed States on Roughened Ag, Au, and Cu Electrode Surfaces at Physiological pH. *J. Phys. Chem. B* **2009**, *113*, 10974−10983.
(51) Ambrosio, R. C.; Gewirth, A. A. Characterization of Water Structure on Silver Electrode Surfaces by SERS with Two-Dimensional Correlation Spectroscopy. *Anal. Chem.* **2010**, *82*, 1305−1310.
(52) Dieringer, J. A.; Lettan, R. B.; Scheidt, K. A.; Van Duyne, R. P. A Frequency Domain Existence Proof of Single-Molecule Surface-Enhanced Raman Spectroscopy. *J. Am. Chem. Soc.* **2007**, *129*, 16249−16256.
(53) Noda, I. *In Handbook of Vibrational Spectroscopy*; Chalmers, J., Griffiths, P., Eds.; John Wiley & Sons: New York, 2002; Vol. *3*.
(54) *Two-Dimensional Correlation Spectroscopy*; Ozaki, Y., Noda, I., Eds.; AIP Conference Proceedings 503; American Institute of Physics: Melville, NY, 2000.
(55) Kitahama, Y.; Ogawa, A.; Tanaka, Y.; Obeidat, S.; Itoh, T.; Ishikawa, M.; Ozaki, Y. Difference in Time Dependence of Surface-Enhanced Raman Scattering Spectra of Thiacarbocyanine J- and H-aggregates Adsorbed on Single Silver Nanoaggregates. *Chem. Phys. Lett.* **2010**, *493*, 309−313.
(56) Talley, C. E.; Jusinski, L.; Hollars, C. W.; Lane, S. M.; Huser, T. Intracellular pH Sensors Based on Surface-enhanced Raman Scattering. *Anal. Chem.* **2004**, *76*, 7064−7068.
(57) Wano, H.; Uosaki, K. In Situ, Real-Time Monitoring of the Reductive Desorption Process of Self-Assembled Monolayers of Hexanethiol on Au(111) Surfaces in Acidic and Alkaline Aqueous Solutions by Scanning Tunneling Microscopy. *Langmuir* **2001**, *17*, 8224−8228.